Soft Matter

Accepted Manuscript

ROYAL SOCIETY OF CHEMISTRY

www.rsc.org/softmatter

Aging mechanism in model Pickering emulsion

Sarah Fouilloux,[a] Florent Malloggi,[a] Jean Daillant,[b] and Antoine Thill[a*]

We study the stability of a model Pickering emulsion system using fluorinated oil and functionnalized silica nanoparticles. A special counter-flow microfluidics set-up was used to prepare monodisperse oil droplets in water. The wettability of the monodisperse silica nanoparticles (NPs) could be tuned by surface grafting and the surface coverage of the droplets was controlled using the microfluidics setup. For surface coverage as low as 23%, we observe a regime of Pickering emulsion stability where the surface coverage of emulsion droplets of constant size increases in time, in coexistence with an excess oil phase. Our results demonstrate that the previously observed limited coalescence regime where surface coverage tends to control the average size of the final droplets must be put in a broader perspective.

1 Introduction

Ramsden[1] and Pickering[2] observed one century ago that solid particles are able to stabilize emulsions, now referred to as Pickering emulsions[3]. Depending on the particles wettability, either O/W emulsions (hydrophilic particles, contact angle $\theta < 90^{\circ}$) or W/O emulsions (hydrophobic particles, $\theta > 90^{\circ}$) are preferably stabilized. The attachment energy of the nanoparticles at the interface is normally large and gets stronger when the nanoparticles get larger. It is usually admitted that NPs of more than 10 nm are irreversibly adsorbed at the oil water interface[4,5] resulting in enhanced stability for instance against dilution. When the proper NPs concentration is used[6], limited coalescence is another attractive characteristic of Pickering emulsions which unable the control of the average size. The total amount of particles initially adsorbed is usually not sufficient to efficiently protect the oil-water interfaces. In such a case, the emulsion droplets coalesce leading to a progressive reduction of the total interfacial area between oil and water interfaces. As particles are irreversibly adsorbed, the reduction in oil/water interfacial area goes along with an increase in surface coverage. The coalescence continues until a surface coverage sufficient to protect the oil/water interface is reached[7].

To progress in our understanding of the stability behavior of Pickering emulsions, we propose to study a model Pickering emulsion with i-controlled sizes of both droplets and NPs ii- controlled hydrophobicity of NPs stabilizers and iii- controlled surface coverage. To succeed, we developed a fluidic system which unabled experimental *in-situ* controlled surface coverage measurements of Pickering emulsion by Small Angle X-rays Scattering (SAXS). The main advantage of *in-situ* measurements is to trully linked the surface coverage to the instability mechanism. To the best of our knowledge, it is the first time that such a study is performed: standard approaches are usually based on making X-rays or neutrons reflectivity in planar surfaces[8,9,10].

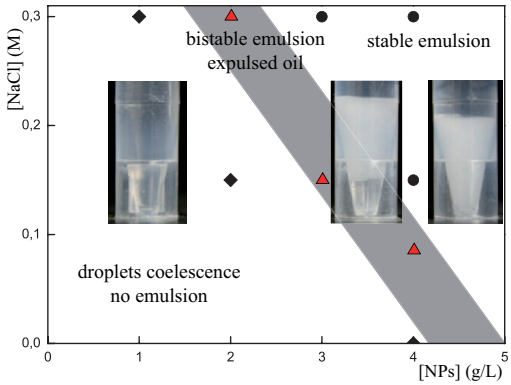

Fig. 1 Phase diagram as a function of the ionic strength and NPs concentration.

The past decade has seen the rise of microfluidic tools, see for a non-exhaustive review[11], that allow, among other, a good control of emulsions, i.e. monodisperse droplets[12] and surface coverage by particles[13,14]. In this article we have set-up a microfluidic system allowing such a coupled control. We produce monodisperse oil-in-water (O/W) droplets stabilized by monodisperse silica NPs. The surface coverage of the droplets by the NPs is controlled through the microfluidic process. Due to the fine controlled of NPs coverage, we are able to determine the stability diagram of the Pickering emulsion (see Fig.1). In addition, we observe a stability regime where a large amount of dispersed phase is expelled while the other oil droplets keep their native size.

[a] *Interdisciplinary Laboratory on Nanoscale and Supramolecular Organizations, CEA-Saclay, IRAMIS/NIMBE/LIONS, UMR CNRS 3685,Gif-sur-Yvette, France.*
[b] *Synchrotron Soleil, Gif-sur-Yvette, France.*
[*] *corresponding author, florent.malloggi@cea.fr*

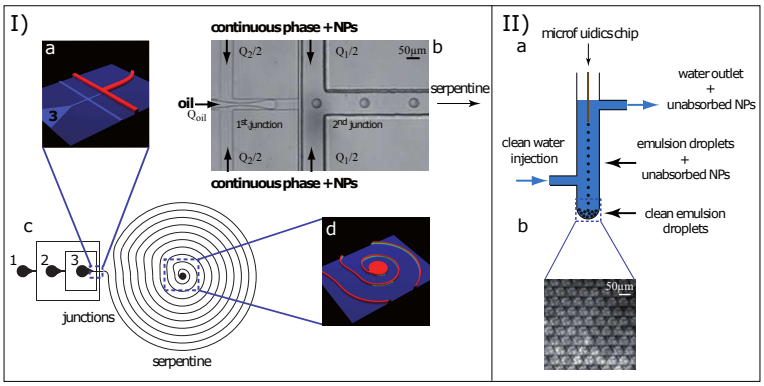

Fig. 2 Microfluidics set-up **I**-Emulsion generator.**a**-**d** 3D profiles of the junctions and the outlet of serpentine of the microfluidics mold obtained from an optical interferemeter. **b** Picture of the droplets formation at the junctions.**c** AutoCAD design of the microfluidics device with the three inlets:1-2 NPs in water (Q_1= 7μl/min ; Q_2= 1.5μl/min) and 3 oil phase (Q_{oil} = 0.3μl/min). **II**-Emulsion cleaner.**a** Sketch of the emulsion cleaner. The Pickering emulsion entered from the top and it is washed by the counter flow. **b** Picture of the clean monodisperse emulsion obtained.

2 Experimental set-up

2.1 Functionalized nanoparticles

Well-controlled silica nanoparticles were prepared according to the method of Fouilloux *et al.*[15] and their surface energy was modified by grafting trimethylethoxysilane (TMES) (Supplementary Material: Nanoparticles preparation). Their size and aggregation state was then assessed with SAXS (Small Angle X-ray Scattering) and DLS (Dynamic Light Scattering) after dialysis. Surface density of silanol functions is determined by titration (total number of silanol functions) and SAXS measurements (total surface of NPs). Bare silica NPs have 4.5 silanol/nm^2. The silanol densities are reduced up to 1 silanol/nm^2 after grafting TMES. Using DLS size measurements, it is observed that up to a total TMES concentration of 4.6 TMES molecules/nm^2 ($\sim$ 3 silanol/nm^2), the surface modified NPs are still well dispersed in water (Supplementary Material: Nanoparticles titration and Surface modification of NPs). SAXS measurements indicate that a repulsive interaction exists between the NPs even after the surface treatment at 4.6 TMES/nm^2. When more than about 8 TMES/nm^2 is used in the surface modification reaction, the NPs are no longer stable in water, but it is still possible to partially disperse the NPs using ethanol as a solvent. In the following we only used NPs dispersed in water.

2.2 Microfluidic droplets generator

The microfluidic device consists of two flows focusing in series (see Fig.2-I) microfabricated using standard multilayers soft technology[16,17]. The first junction (width 50 μm and height 11 μm) generates the oil droplets: the dispersed phase (fluorinated oil) is sheared by the continuous phase (water + NPs) until the interface destabilization. Once the droplets are formed they flow to the second junction. In order to optimize the NPs adsorption the second junction (two steps lithography[18]) has a larger width (100 μm) and height (95 μm). In such larger channel, the droplets adopt a 3D shape (sphere of radius 22μm) and are fully surrounded by NPs. To maximize the contact time of NPs with the oil droplets, we make a 40 cm long serpentine which, according to the flow rate we fixed (Q_{oil}=0.3μl/min, $Q_{cont.phase}$ = 8.5μl/min), gives a resident time of 27s. The Stokes-Einstein formula gives a diffusion coefficient D = 3.1$\times 10^{-11}$ m^2.s^{-1} (NPs of radius 7.1 nm) and the mean transverse diffusion length writes $l = \sqrt{2Dt} = 40\mu m$. Hence almost all the NPs entered at the 2nd junction reach the droplet interface at the end of the serpentine (the maximal lateral diffusion length is 50μm when no droplet is in the channel and 30μm with droplets). Another parameter to adjust is the number of NPs in contact with the oil droplets. We used concentrations of NPs that range from 0.4 to 3.5 g.L^{-1}. In many cases, a NaCl salt concentration of up to 0.3M was used to screen the repulsive electrostatic repulsions between the NPs. We checked that NPs do not aggregate at such a high ionic strength (data not shown). At the outlet of the microfluidic chip, only part of the injected NPs are adsorbed at the oil interface. The emulsion droplets coexist with a suspension of unabsorbed NPs. In order to remove the excess NPs, the outlet of the microfluidics is connected to a rinsing millifluidic set-up (Figure 2-II). It consists of a homemade glass vial with one inlet (linked to the microfluidics device) and two lateral connections. A pure Millipore water flows from bottom to top through the lateral connections. The emulsion droplets enter from the top of the vial and fall in a clean water counter flow. The fluorinated oil density (1.82 g/cm^3) guarantees that the droplets will settle even in a significant counter flow. **The non-adsorbed NPs are thus removed from the emulsion suspension**. At the bottom of the set-up, only the NPs previously adsorbed at the interface of the oil droplet will remain (see the emulsion crystal-like structure in Figure02-IIb). Hence the use of variable NPs concentrations allows producing Pickering emulsions with a tuned surface NPs coverage.

2.3 Pickering emulsion

To produce the emulsions in the microfluidic device, we have selected a surface modification which guarantees a colloidal stability in water. The NPs with 70% residual silanol surface groups ($\sim$3 silanol/nm^2) were introduced at concentrations of 1, 1.7 and 3.5 g.L^{-1} in the presence of 0.3M NaCl. This salt concentration is enough to almost completely screen the repulsive interaction

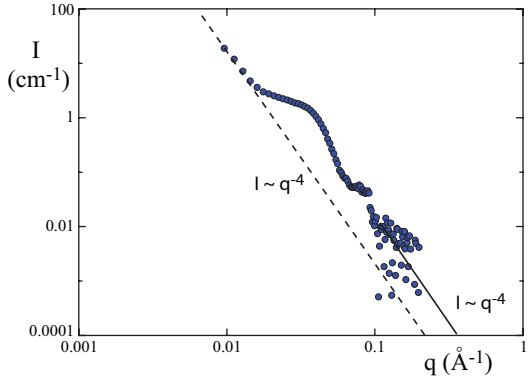

Fig. 3 SAXS measurements of an oil-in-water emulsion stabilized with monodisperse silica NPs. The excess NPs have been removed by counter flow rinsing before collection of the droplets. The full line represents the Porod extrapolation of the NPs and the dotted line the Porod extrapolation of the oil droplets.

between the NPs. However, the aggregation kinetic of the NPs is very slow compared to the resident time in the fluidic system (∼30s). This guarantees that only isolated NPs are in contact with the oil/water interface in the chip. According to the droplet emulsion conditions (Q_{oil}=0.3μl/min and radius=22μm) the oil surface produced is 4×10^{-5} m^2/min. At the lowest NPs concentration of 0.4 g.L^{-1}, the available NPs cross section is 1.6×10^{-4} m^2/min. Therefore the NPs available to cover the oil droplets are at least 4 times larger than the oil area created within the emulsion. The diffusion-convection characteristics of the NPs in the microchannel flow together with the residual electrostatic repulsive interactions however prevent from reaching a full coverage of the droplets at the chip outlet for the lowest concentration. The NPs concentration is thus introduced in large excess in order to force significant adsorption within the available contact time and the excess NPs is removed in the millifluidic counter flow device.

2.4 Surface coverage measurements

SAXS is an ideal technique for probing the size, shape, polydispersity and concentration on particles *in situ*. It is especially valuable when particles have sizes in the nanometer range [19,20]. Moreover the surface coverage of the droplets can be determined through model-independent analysis of the SAXS intensity (See supporting Information for details). In the case where the scatterers have a sharp well-defined interface with the surrounding medium, the scattered intensity will follow a q^{-4} slope in the large scattering vector range. This regime, called Porod regime give a finite value for $\lim_{q\to+\infty} q^4 I(q)$ which is proportional to the surface area of the scattering phase. We used a second model-independent property of the scattered intensity called the invariant Q. Indeed, $Q = \int_0^{+\infty} q^2 I(q) dq$ is a constant which only depends on the volume fractions and scattering length densities of the scattering objects (see eq. 5 in S.I.).

In our experiments, some emulsions were collected directly in a glass capillary for SAXS analysis. The capillary is connected to the bottom of the millifluidic rinsing device: the emulsion collected in the SAXS capillary only contain partially covered oil droplets without an excess of free NPs. Figure 3 shows SAXS measurements for an emulsion prepared with the 7.5 nm NPs having 70% residual silanol groups on their surface at a concentration of 1 g.L^{-1} in the presence of 0.3M NaCl.

In the very low q range (q∼0.01Å^{-1}), the scattered intensity follows a q^{-4} Porod regime which is proportional to the oil/water interface. In the intermediate q range, the scattered intensity is due to the presence of the adsorbed NPs and at the large q range (q>0.1Å^{-1}) there is a second q^{-4} Porod regime which is proportional to the quantity of NPs present at the interface. Comparing the two Porod regimes together with the computation of Q, we deduce the NPs volume fraction Φ_{NP} in the sample (for data treatment details see Supplementary Material: Analysis of SAXS measurements). As both the sizes of the droplets and NPs is well-defined, the surface coverage is deduced using $\tau = \Phi_{NP} R / 4\Phi_0 r$ where r and R are the radius of the NPs and droplets respectively and Φ_0 is the oil volume fraction.

3 Results

The Figure 4 shows the surface coverage τ for three different initial NPs concentrations (1, 1.7 and 3.5 g.L^{-1}) in the presence of 0.3M NaCl, which were measured immediately after preparation and also after several days of aging time up to about one week. The initial surface coverage of the oil droplets appears to be significantly dependent on the NPs initial concentration. The surface coverages measured immediately after the sample preparation are 24 ± 3 % for 1g.L^{-1}, 53 ± 6.6 % for 1.7 g.L^{-1} and 77 ± 9.6 % for 3.5 g.L^{-1}. The contact time with the NPs is the same for all concentrations: the surface coverage is efficiently controlled by the NPs concentration in the continuous phase. The need to use a large excess of NPs to control the coverage is not a problem when the excess NPs is removed before analysis. Experiments (not shown) were the excess NPs is not removed immediately show an equivalent coverage of ∼80% and stable emulsions whatever the NPs concentrations. The rinsed emulsions having various initial surface coverage show interesting aging behavior. The emulsions prepared with the highest NPs concentration have an initial surface coverage of ∼75%. This coverage appears to be stable over time. The emulsion appears also stable macroscopically. On the contrary, a change in the surface coverage is observed for

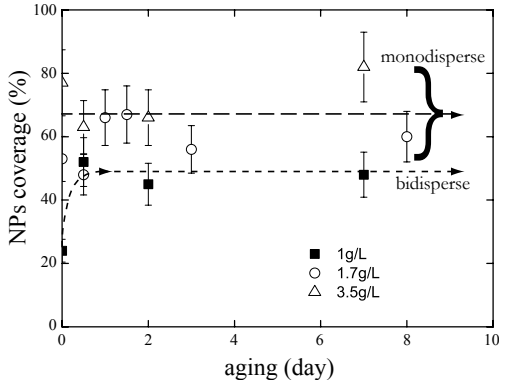

Fig. 4 Surface coverage of the microfluidic prepared emulsions as a function of aging time for three NPs initial concentrations.

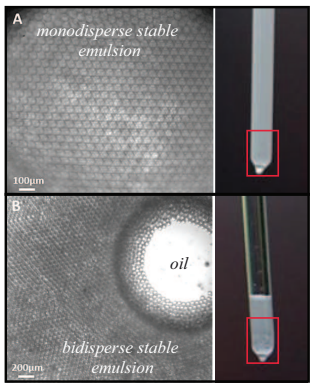

Fig. 5 Microscope image of the Pickering emulsions after one day aging. **A**. Initial surface coverage >50%. **B**. Initial surface coverage ∼25%.

emulsions prepared with the lowest concentrations experiment. The initial coverage is slightly above 20% but it rapidly increases up to about 50% after only 1 day. Macroscopically, the emulsion is not as stable as the one prepared with a high NPs concentration: we observe an excess of oil (big droplets) coexisting with the native emulsion droplets. The Figure 5 shows such a rinsed emulsion observed with an optical microscope one day after the formation. It is clear that for emulsions with initial surface coverage above 50% (Fig.5-A) oil droplets are stable whereas in the case of initial surface coverage of 24% (Fig.5-B) big oil droplets co-exist with native one. This excess oil was not present after the emulsion rinsing step.

4 Discussion

In the following we discuss this new result and we propose a scenario for this excess oil expulsion. At the outlet of the microfluidic chip, all droplets have the same diameter. If we neglect Oswald ripening and if we assume that NPs are conserved upon coalescence (*i.e.* no NPs are expelled from the interface), we write the droplet size emulsion $R = R_i\sqrt[3]{n}$, the number of adsorbed NPs $N = n4\pi {R_i}^2\tau_i/\pi r^2$ and the surface coverage[21] $\tau = \tau_i\sqrt[3]{n}$ as a function of the initial droplet size R_i, the initial surface coverage τ_i and the number of coalescence events n. According to the results shown is Fig.4, when 1 g.L^{-1} NPs suspension is used to stabilize the droplets, the initial surface coverage τ_i is 23%. After one day of aging, the surface coverage increased up to $\tau = 50\%$ and stays almost constant. If we assume no NPs expulsion from the oil/water interface, the final droplet size would writes $R_n = R_i\tau_n/\tau_i$ which gives $R_n = 43\ \mu m$. This scenario is not what we have as confirmed by the pictures on Fig.5-B. Indeed,we see particles with the initial size ($\sim 20\mu m$). Hence some NPs have been added to the surface of droplets without coalescence events. As excess oil has appeared, we make the following hypothesis to explain our observation. The 23% surface coverage corresponds to a surface coverage where rare coalescence events remain possible. Contrarily to the limited coalescence, we suppose that a significant part of the NPs adsorbed on the droplets are released in the suspension upon coalescence. In such a scenario, coalescence may not be a stabilizing mechanism but could become a catastrophic event which further increases the coalescence probability for the droplet if the surface coverage after coalescence is less than before.

To go a step further in the destabilization mechanism comprehension, we make an energetic balance between adhesion energy and gain in interfacial energy to check against the validity of our assumption.

NPs Energy adhesion. The adsorption of partially wetted NPs is often believed to be irreversible as soon as their size is close to 10 nm or more. The adhesion energy per NPs[22,23,24,25] is indeed given by $E_{ad} = \pi r^2\gamma(1 \pm cos\theta)^2$with r the radius of NPs, γ the interfacial energy of oil/water and θ the contact angle of NPs at the oil/water interface. In this study, we have used silica NPs having a size of r=7.1 nm and at least 70% of their silanol surface sites. Binks *et al.*[26] have proposed computed contact angle as a function of the residual silanol groups at the surface of silica NPs. For 75% SiOH, they predict a contact angle $\theta = 65^\circ$for γ =50 mN/m. In such a condition and with a NP of radius r=7.1 nm this gives almost $E_{ad} = 700k_BT$ where k_BT is the product of Boltzmann's constant and the absolute temperature $T = 298K$. According to this estimation it is clear that, once adsorbed at the oil/water interface, NPs will not escape through only thermal activation.

Energy released during coalescence events. Upon coalescence the droplet released part of their interfacial energy due to the decrease of oil/water interface. The variation of interfacial energy ΔE of two droplets (initial radius R and area $2S = 2\times 4\pi R^2$) coalescing into a final droplet (radius R_f and an area $S_f = 4\pi R_f^2$) writes:

$$\Delta E = \gamma(S_f - 2S) = 4\pi\gamma(R_f^2 - 2R^2) = 2(2^{-1/3} - 1)4\pi R^2\gamma \qquad (1)$$

If we compare the excess interfacial energy per adsorbed NPs i.e. $\Delta E/N$ with $N = 2\times 4\pi R^2\tau/\pi r^2$ where τ is the initial surface coverage and N the number of NPs of the two droplets, to the adhesion energy E_{ad}, we obtain the ratio:

$$\alpha = \frac{\Delta E}{NE_{ad}} = \frac{2^{-1/3} - 1}{(1 - cos\theta)^2\tau} \qquad (2)$$

For NPs having a contact angle of 65°, the energy ratio is simply $\alpha \sim -0.62/\tau$. With an initial surface coverage of τ= 0.23, the gain of interfacial energy per NPs is 2.7 times more than the adhesion energy. The surface coverage stabilizes at $\tau \sim$0.65-0.7 which corresponds to the point where the interfacial energy gain per NPs upon coalescence is no longer superior to the adhesion energy. This simple energetic comparison is just intended to show that the assumption of a NPs release upon coalescence of a Pickering emulsion may not be an impossible process. Surprisingly in this case, this simple calculation seems also to correspond to the stabilization process of the droplets. However the precise energetic transferred to the NPs remain unclear as part of the energy is used to move fluids. In our case, the fluorinated oil has a very low viscosity which is favorable to transfer more energy to the NPs.

5 Conclusions

In conclusion, we have built a new and original coupled microfluidic/millifluidic system to prepare model Pickering emulsions. The droplets are stabilized by monodisperse NPs having controlled surface properties. This set-up allows tuning the surface coverage of the final emulsion by changing the NPs concentration in the microfluidic system. The obtained surface coverage is experimentally determined *in situ* using SAXS measurements of the as prepared emulsion. This technique does not require any manipulation of the sample. It has been thus possible to follow the aging of emulsions having varying initial surface coverage from 23% to 77%. We have identified two stability scenarios depending on the initial emulsion surface coverage. For the highest surface coverage (>50%), the emulsion remain monodisperse and stable for more than one week. For the lowest surface coverage (<50%), an excess disperse phase appear and coexists with almost undisturbed droplets. This destabilization does not follow the partial coalescence pathway. We propose that the transition from limited coalescence and the observed destabilization could be due to a coalescence induced release of NPs. We argue that this process is energetically plausible and that the comparison of the interfacial energy release per adsorbed NPs compared to their adhesion energy could be a guide to understand Pickering emulsion stabilization and aging.

ACKNOWLEDGMENTS. This project has benefited from the support of the Cnano Ile de France grant SINSEM. The Ile de France region is acknowledged for its support of the SEM apparatus used for the NPs imaging and Mathieu Pinault and AurÃľlie Habert for their help.

References

1 W. Ramsden, PROCEEDINGS OF THE ROYAL SOCIETY OF LONDON, 1903, **72**, 156–164.
2 S. Pickering, JOURNAL OF THE CHEMICAL SOCIETY, 1907, **91**, 2001–2021.
3 B. Binks and S. Lumsdon, Langmuir, 2000, **16**, 8622–8631.
4 B. Binks and S. Lumsdon, Langmuir, 2001, **17**, 4540–4547.
5 K. Du, E. Glogowski, T. Emrick, T. P. Russell and A. D. Dinsmore, Langmuir, 2010, **26**, 12518–12522.
6 J. Frelichowska, M.-A. Bolzinger and Y. Chevalier, Journal of Colloid and Interface Science, 2010, **351**, 348–356.
7 S. Arditty, C. Whitby, B. Binks, V. Schmitt and F. Leal-Calderon, European Physical Journal E, 2003, **11**, 273–281.
8 Y. Lin, A. Boker, H. Skaff, D. Cookson, A. Dinsmore, T. Emrick and T. Russell, Langmuir, 2005, **21**, 191–194.
9 J. Reguera, E. Ponomarev, T. Geue, F. Stellacci, F. Bresme and M. Moglianetti, Nanoscale, 2015, **7**, 5665–5673.
10 A.-L. Fameau, J.-P. Douliez, F. BouÃČÂľ, F. Ott and F. Cousin, Journal of Colloid and Interface Science, 2011, **362**, 397 – 405.
11 T. Squires and S. Quake, REVIEWS OF MODERN PHYSICS, 2005, **77**, 977–1026.
12 P. Garstecki, H. Stone and G. Whitesides, Physical Review Letters, 2005, **94**, year.
13 A. R. Studart, H. C. Shum and D. A. Weitz, JOURNAL OF PHYSICAL CHEMISTRY B, 2009, **113**, 3914–3919.
14 S.-H. Kim, S.-J. Jeon, G.-R. Yi, C.-J. Heo, J. H. Choi and S.-M. Yang, Advanced Materials, 2008, **20**, 1649+.
15 S. Fouilloux, A. Desert, O. Tache, O. Spalla, J. Daillant and A. Thill, JOURNAL OF COLLOID AND INTERFACE SCIENCE, 2010, **346**, 79–86.
16 Y. Xia and G. Whitesides, ANGEWANDTE CHEMIE-INTERNATIONAL EDITION, 1998, **37**, 550–575.
17 B. Ziaie, A. Baldi, M. Lei, Y. Gu and R. Siegel, ADVANCED DRUG DELIVERY REVIEWS, 2004, **56**, 145–172.
18 F. Malloggi, N. Pannacci, R. Attia, F. Monti, P. Mary, H. Willaime, P. Tabeling, B. Cabane and P. Poncet, Langmuir, 2010, **26**, 2369–2373.
19 H. Boukari, J. Lin and M. Harris, Journal of Colloid and Interface Science, 1997, **194**, 311–318.
20 K. Larson-Smith, A. Jackson and D. C. Pozzo, Langmuir, 2012, **28**, 2493–2501.
21 J. H. Clint and S. E. Taylor, Colloids and Surfaces, 1992, **65**, 61 – 67.
22 J. H. Clint and N. Quirke, Colloids and Surfaces A: Physicochemical and Engineering Aspects, 1993, **78**, 277 – 278.
23 J. H. Clint, Current Opinion in Colloid and Interface Science, 2001, **6**, 28 – 33.
24 S. Levine, B. D. Bowen and S. J. Partridge, Colloids and Surfaces, 1989, **38**, 325 – 343.
25 R. Aveyard, B. P. Binks and J. H. Clint, Advances in Colloid and Interface Science, 2003, **100âĂŞ102**, 503 – 546.
26 B. Binks and J. Clint, Langmuir, 2002, **18**, 1270–1273.